



ELSEVIER

Journal of Alloys and Compounds 335 (2002) 191–195

Journal of
ALLOYS
AND COMPOUNDS

www.elsevier.com/locate/jallcom

Solid solution range of boron and properties of the perovskite-type NdRh_3B

Toetsu Shishido^{a,*}, Takahiko Sasaki^a, Kunio Kudou^b, Shigeru Okada^c, Akira Yoshikawa^a,
Jung Min Ko^a, Jinhua Ye^d, Iwami Higashi^e, Masaoki Oku^a, Hiroyuki Horiuchi^f,
Tsuguo Fukuda^a, Shigemi Kohiki^g, Kazuo Nakajima^a

^aInstitute for Materials Research (IMR), Tohoku University, 2-1-1 Katahira, Aoba-ku, Sendai 980-8577, Japan

^bDepartment of Mechanical Engineering, Kanagawa University, 3-27-1 Rokkakubashi, Kanagawa-ku, Yokohama 221-8686, Japan

^cDepartment of Civil Engineering, Faculty of Engineering, Kokushikan University, 4-28-1, Setagaya-ku, Tokyo 154-0017, Japan

^dNational Institute for Materials Science, 1-2-1 Sengen, Tsukuba, Ibaraki 305-0047, Japan

^eDepartment of Chemistry, Chiba Institute of Technology, Shibazono, Narashino, Chiba 275-0023, Japan

^fEarth Science Laboratory, Faculty of Education, Hirosaki University, 1 Bunkyo-cho, Hirosaki, Aomori 036-8560, Japan

^gThe Kyusyu Institute of Technology, Kita-kyusyu 804-8550, Japan

Received 27 April 2001; received in revised form 13 July 2001; accepted 24 July 2001

Abstract

Polycrystalline samples of NdRh_3B_x have been synthesized by arc melting technique. The crystal structure of NdRh_3B_x is the perovskite-type cubic system (space group $Pm\bar{3}m$) for nominal boron concentration in the range of $0.706 \leq x \leq 1.000$ (15–20 mol.% B). The lattice parameter a varies linearly from 0.41749(7) nm ($x=0.706$) to $a=0.42136(6)$ nm ($x=1.000$). Thermogravimetric analysis indicates that the oxidation onset temperature for $\text{NdRh}_3\text{B}_{1.000}$ is 663 K. The weight gain of the sample by heating in air up to 1473 K is 10.00% for $\text{NdRh}_3\text{B}_{1.000}$, and oxidized products are Rh and NdBO_3 . The micro-Vickers hardness is 4.9 ± 0.05 GPa for $\text{NdRh}_3\text{B}_{1.000}$. $\text{NdRh}_3\text{B}_{1.000}$ shows a metallic temperature dependence of the resistivity down to 0.5 K. Magnetic susceptibilities for $\text{NdRh}_3\text{B}_{1.000}$ show Curie-like paramagnetic temperature dependence due to Nd^{3+} moments. No trace of magnetic phase transitions and superconductivity is found. © 2002 Elsevier Science B.V. All rights reserved.

Keywords: NdRh_3B ; Microhardness; Oxidation resistance in air; Electric property; Magnetic property

1. Introduction

The rare earth element (RE)–platinum group element–boron (B) systems have received considerable attention from many researchers in the fields of crystallography, magnetism, superconductivity, heavy-electron behaviour and valence fluctuations. Particularly, the discovery of the ErRh_4B_4 compound, which is a re-entrant superconductor, has drawn much attention to these ternary systems [1,2]. We have previously prepared single crystals of several compounds by molten metal flux method, using Cu as a flux. They are ErRh_3B (cubic system, space group: $Pm\bar{3}m$, $a=0.4146$ nm), ErRh_3B_2 (base-centered monoclinic system, ErIr_3B_2 type, space group: $C2/m$, $a=0.5355(1)$ nm, $b=0.9282(1)$ nm, $c=0.3102(1)$ nm, $\beta=90.89(3)^\circ$) and

ErRh_4B_4 (simple tetragonal system, space group: $P4_2/mc$, $a=0.5304(1)$ nm, $c=0.7395(2)$ nm). The physical and chemical properties of these crystals have been reported [3,4].

Many studies of perovskite-type oxides have been performed due to the interesting features in the superconducting transition, the insulator–metallic transition, ion conduction characteristics, dielectric properties, and ferroelasticity. On the other hand, there have been few studies on non-oxide perovskite-type compounds [5,6].

We have previously prepared RERh_3B (RE=La, Gd and Lu) by arc-melting synthetic method [7,8], where La, Gd and Lu are the first, middle and last elements of the lanthanoids, in which RE is positioned at the eight corners of the cube, Rh is face-centered and B is body-centered. The B-deficient compounds, RERh_3B_x , can also be obtained. The B content variation induces changes in the electromagnetic properties, hardness, and chemical resistance against oxidation in air at high temperature.

*Corresponding author. Tel.: +81-22-215-2233; fax: +81-22-215-2202.

E-mail address: crystal@imr.tohoku.ac.jp (T. Shishido).

In this study, we focused on the less than half element of Nd (atomic number 60) in the lanthanoids. We synthesized the perovskite-type compound NdRh_3B_x . The solid solution range of boron in the NdRh_3B_x is clarified by powder X-ray diffraction (XRD) analysis, and the variation of the lattice constant of the sample is investigated as a function of the boron concentration x . Vickers microhardness (H_v) and thermogravimetric and differential thermal analysis (TG–DTA) measurements were performed on the samples. The temperature dependence of the electrical resistance and magnetization was studied for the samples.

2. Experimental

2.1. Sample preparation

Polycrystalline samples of NdRh_3B_x were synthesized by the arc melting method using 99.9% pure Nd, Rh and B as raw materials. These were weighed in the atomic ratio 1:3: x , where $x=1.000$ (20 mol.% B), 0.848 (17.5 mol.% B), 0.706 (15 mol.% B), 0.444 (10 mol.% B), 0.210 (5 mol.% B) and 0 (0 mol.% B). The mixture of the starting materials, about 2 g for each sample, was placed in a water-cooled copper hearth in a reaction chamber. Argon was used as a protective atmosphere. The pressure inside the chamber was ~ 1 atm. A small amount of residual oxygen in argon was eliminated by fusing a button of titanium as a reducing agent. The starting materials were then melted for 3 min by an argon arc plasma flame with DC power source at 20 V and 100 A. The samples were then turned over and melted three times under the same conditions. Finally, synthesized samples were wrapped in tantalum foil and annealed at 1573 K for 20 h under vacuum to ensure homogeneity.

2.2. Characterization

For chemical analysis, the samples were fused using NaHSO_4 as a flux reagent, then the obtained material was dissolved into HCl. The chemical composition of each solution was analyzed by the induction coupled plasma atomic emission spectrometry (ICP–AES) method, using Zn as internal standard. Crystal structure characterization of the samples was performed by XRD. The micro-Vickers hardness for the samples was measured at room temperature. A load of 100 g was applied for 15 s and 10 impressions were recorded for each sample. The obtained values were averaged and the experimental error was estimated. Thermogravimetric analysis and differential thermal analysis were performed between room temperature and 1473 K to study the oxidation resistance of the samples in air. A sample was heated at a rate of 10 K/min up to 1473 K. The oxidation products were analyzed by powder X-ray diffractometry. The electrical resistivity of the samples was measured by means of a DC four probe

method from 0.5 K to room temperature. The magnetic susceptibility measurements were performed in a field of 5000 Oe using a commercial SQUID magnetometer (Quantum Design Inc., MPMS-5) from 5 K to room temperature.

3. Results and discussion

3.1. Appearance and chemical composition of synthesized material

Since the boiling points of Nd, Rh and B are high at 3373, 4233 and 2823 K, respectively, evaporation can be neglected [9]. Accordingly, we judge that the arc melting method is suitable for the synthesis of NdRh_3B_x . Samples of NdRh_3B_x obtained by varying the B content x were all silver in color and exhibited a metallic lustre. The result of chemical analysis shows that the chemical compositions before and after synthesis are almost the same. In addition, contamination from the electrode (tungsten) and hearth (copper) could be disregarded in this study.

3.2. Relationship between the nonstoichiometry of B and the lattice constant of NdRh_3B_x samples

The crystal structure analysis on NdRh_3B_x samples with a B content of $x=1.000$ by powder XRD reveals that it is a perovskite-type compound (space group: $Pm\bar{3}m$) in which Nd is positioned at the eight corners of the cube, Rh is face-centered and B is body-centered (Fig. 1). By varying x , the nonstoichiometry of B and the resulting change of the crystal structure were studied. Fig. 2 shows changes of

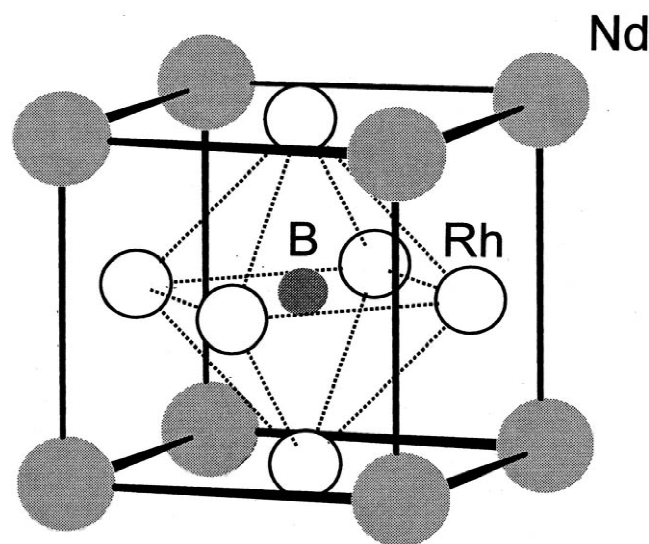


Fig. 1. Arrangement of atoms in the perovskite-type NdRh_3B . Large gray, large open and small black circles represent Nd, Rh and B atoms, respectively.

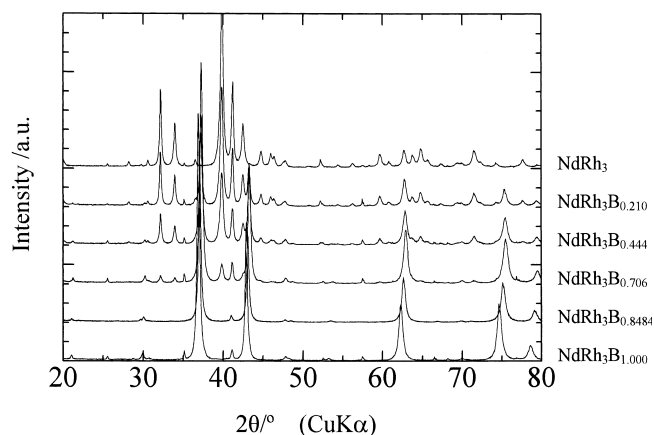


Fig. 2. Powder XRD profiles for NdRh_3B_x with $x=1.000$, $x=0.8484$, $x=0.706$, $x=0.444$, $x=0.210$ and $x=0$. These are nominal compositions. In the cases of $x=0.706$, $x=0.444$ and $x=0.210$, a mixture phase of NdRh_3B_x and NdRh_3 is formed.

the powder XRD patterns when x is varied. With decreasing x , the XRD peaks of the perovskite-type phase are shifted to higher angles. In the cases of $x=0.706$, 0.444 and 0.210 , two phases of NdRh_3B_x and NdRh_3 are observed.

Fig. 3 shows the relationship between x and the lattice constant of NdRh_3B_x . The lattice constant changes almost linearly with x , varying from $0.41749(7)$ nm ($x=0.706$) to $0.42136(6)$ nm ($x=1.000$). Table 1 shows the lattice parameters of the NdRh_3B_x . Accordingly, NdRh_3B_x exists in a nonstoichiometric range of $0.706 \leq x \leq 1.000$. Mean-

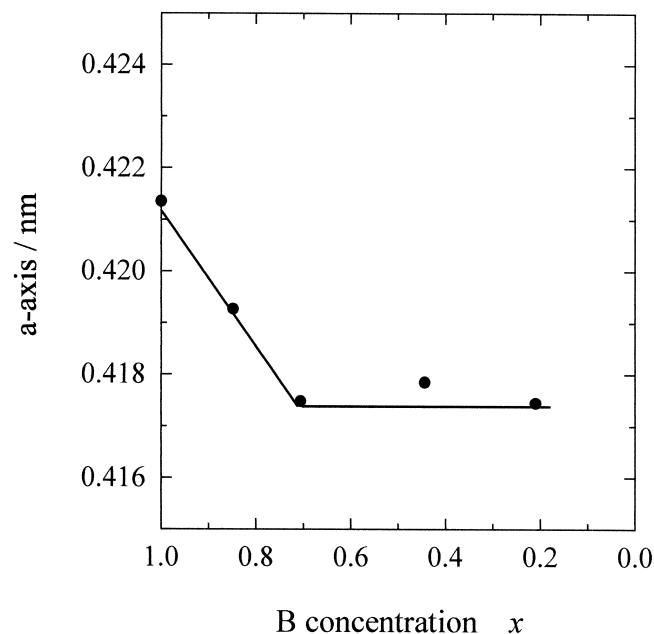


Fig. 3. The variation of lattice constant a as a function of boron concentration x in NdRh_3B_x .

Table 1
Lattice parameter of the NdRh_3B_x

Sample (at.% of boron)	Lattice parameter a , nm	Error nm
$\text{NdRh}_3\text{B}_{1.000}$ (20)	0.41236	0.00006
$\text{NdRh}_3\text{B}_{0.848}$ (17.5)	0.41927	0.00008
$\text{NdRh}_3\text{B}_{0.706}$ (15)	0.41749	0.00007
$\text{NdRh}_3\text{B}_{0.444}$ (10)	0.4179	0.0001
$\text{NdRh}_3\text{B}_{0.210}$ (5)	0.4175	0.0001

while, according to our experimental results for LaRh_3B_x , the perovskite-type compound does not have B-nonstoichiometry, which indicates that $x=1$. In the case of GdRh_3B_x and LuRh_3B_x , B-nonstoichiometry ranges within $0.55 \leq x \leq 1.00$ and $0.30 \leq x \leq 1.00$, respectively. The aforementioned results are listed in Table 2. As shown in Table 2, B exhibits no nonstoichiometry in the case of RE=La. La has the largest atomic radius among all the RE elements, while B gradually became nonstoichiometric as the atomic radius is decreased in the order of Nd, Gd and Lu. Electronegativity of the RE elements changes from 1.1 (La) to 1.2 (Lu). Electronegativity of the RE atoms seems to also affect boron nonstoichiometry of the RERh_3B_x .

3.3. Relationship between B content and hardness in NdRh_3B_x

We studied the hardness of NdRh_3B_x , which reflects the nature of the chemical bonding. Table 3 shows that the microhardness of the compound is 4.3 ± 0.2 and 4.9 ± 0.05 GPa when $x=0.848$ and 1.000 , respectively. In a previous

Table 2
Boron nonstoichiometry in the RERh_3B_x (RE=La, Nd, Gd, Lu)

RERh_3B_x	Boron nonstoichiometry range of x	Reference
La	$x=1$	[8]
Nd	$0.71 \leq x \leq 1$	This study
Gd	$0.55 \leq x \leq 1$	[7]
Lu	$0.30 \leq x \leq 1$	[8]

Table 3
Vickers hardness of the NdRh_3B_x

Sample (at.% of boron)	Hardness, GPa
$\text{NdRh}_3\text{B}_{1.000}$ (20) ^a	4.9 ± 0.05
$\text{NdRh}_3\text{B}_{0.848}$ (17.5) ^a	4.3 ± 0.2
RhB (50) ^b	12.1
Rh_7B_3 (30) ^b	7.8

^a Cubic system.

^b Hexagonal system.

study, as shown in Table 3, the value of microhardness for an Rh–B binary system increased with boron content of the compound [10]. This tendency of binary borides is essentially in agreement with our data on ternary borides. We then focused on only stoichiometric $\text{RERh}_3\text{B}_{1.000}$. The hardness in the series of $\text{RE}=\text{La}, \text{Nd}, \text{Gd}$ and Lu is listed in Table 4. Hardness increases with decreasing atomic size of the RE in $\text{RERh}_3\text{B}_{1.000}$; it became greater with increasing density of itself. In all cases of $\text{RE}=\text{La}, \text{Nd}, \text{Gd}$ and Lu , hardness of the compound decreases with decreasing the boron content x in RERh_3B_x . In GdRh_3B_x , for example, boron nonstoichiometry ranges between $0.55 \leq x \leq 1$ and hardness changes from 4.0 ± 0.1 to 6.8 ± 0.1 GPa, respectively.

3.4. Resistance to oxidation of $\text{NdRh}_3\text{B}_{1.000}$

We studied how the resistance to oxidation in air, which reflects the nature of the chemical bonds of the compound, varied with the B content. Samples were heated up to 1473 K in air and subjected to thermogravimetric and differential thermal analyses (TG–DTA). As shown in Fig. 4, TG analysis reveals that oxidation begins at 663 K. Maximum weight gains due to oxidation are 11.76% at 1223 K. Final weight gains are 10.00% at 1473 K. A volatile matter, for example B_2O_3 , seems to be formed above 1223 K. DTA reveals exothermic peaks at 823 and 927 K. A study of oxidized products by the powder XRD method shows that the products are Rh and NdBO_3 . The results of TG–DTA are listed in Table 5.

3.5. Resistivity and magnetic susceptibility of $\text{NdRh}_3\text{B}_{1.000}$

Fig. 5 shows the temperature dependence of the electric resistivity of $\text{NdRh}_3\text{B}_{1.000}$. The sample measured exhibits metallic behaviour from room temperature down to 0.5 K. No superconductivity appears at the lowest temperature. Fig. 6 shows the temperature dependence of the magnetization of $\text{NdRh}_3\text{B}_{1.000}$ in a field $H=5000$ Oe. Magnetic susceptibilities for $\text{NdRh}_3\text{B}_{1.000}$ show Curie-like paramagnetic behavior. No trace of magnetic phase transitions and superconductivity is found down to 0.5 K. The inset shows the linear temperature dependence of the inverse susceptibility. The effective Bohr magneton is

Table 4
Vickers hardness of the $\text{RERh}_3\text{B}_{1.000}$

Sample	Hardness GPa	Atomic radius of RE (nm)	Density g/cm^3	Reference
$\text{RERh}_3\text{B}_{1.000}$				
La	4.2 ± 0.1	0.188	9.91	[8]
Nd	4.9 ± 0.05	0.182	10.30	This study
Gd	6.8 ± 0.1	0.180	10.82	[7]
Lu	7.7 ± 0.5	0.174	11.69	[8]

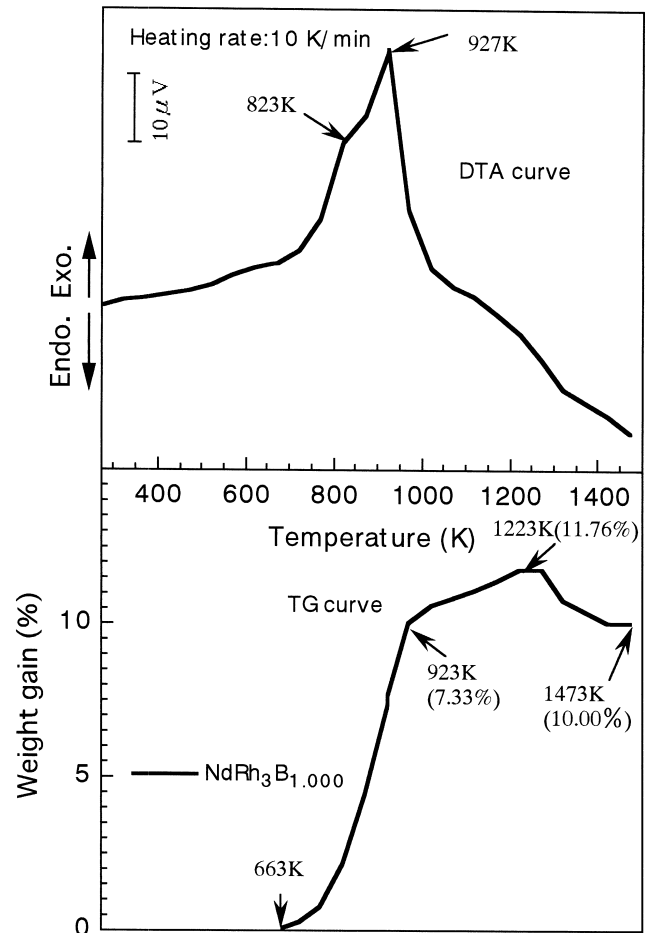


Fig. 4. TG–DTA curves for $\text{NdRh}_3\text{B}_{1.000}$.

calculated to be about 3.5 from the initial slope. This value is close to the theoretical one (3.62) of Nd^{3+} ion.

4. Conclusions

1. Polycrystalline samples of NdRh_3B_x have been synthesized by arc melting method.
2. The structure of the $\text{NdRh}_3\text{B}_{1.000}$ is the perovskite-type cubic system (space group $Pm\bar{3}m$) and this phase exists in the range of $0.706 \leq x \leq 1.000$ (15–20 at.% B). The lattice parameter a varies linearly from $0.41749(7)$ nm ($x=0.706$) to $a=0.42136(6)$ nm ($x=1.000$).
3. By means of TG–DTA between room temperature and 1473 K, the oxidation of the compound in air starts at

Table 5
Results of the TG–DTA measurements for the $\text{NdRh}_3\text{B}_{1.000}$

Sample	Oxidation onset (K)	Exotherm maximum (K)	Weight gain (%)	Oxidation products
$\text{NdRh}_3\text{B}_{1.000}$	663 K	823, 927	10.00	Rh + NdBO_3

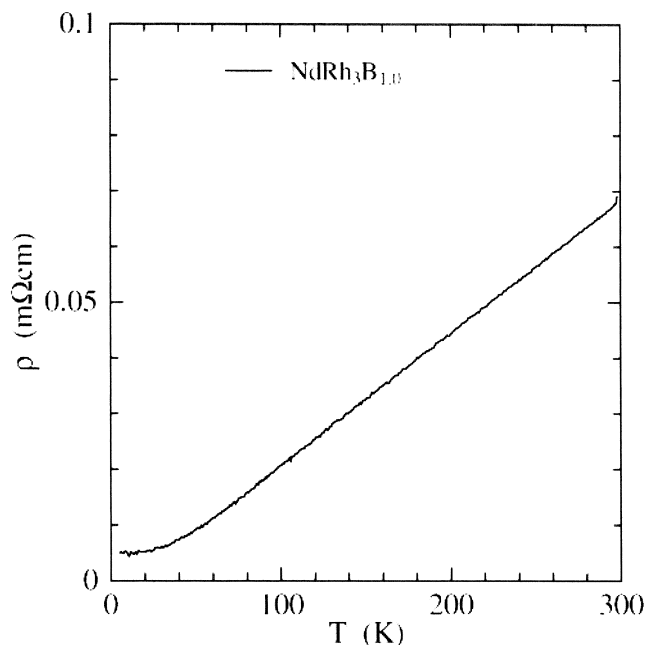


Fig. 5. Temperature dependence of the electric resistivity of $\text{NdRh}_3\text{B}_{1.000}$.

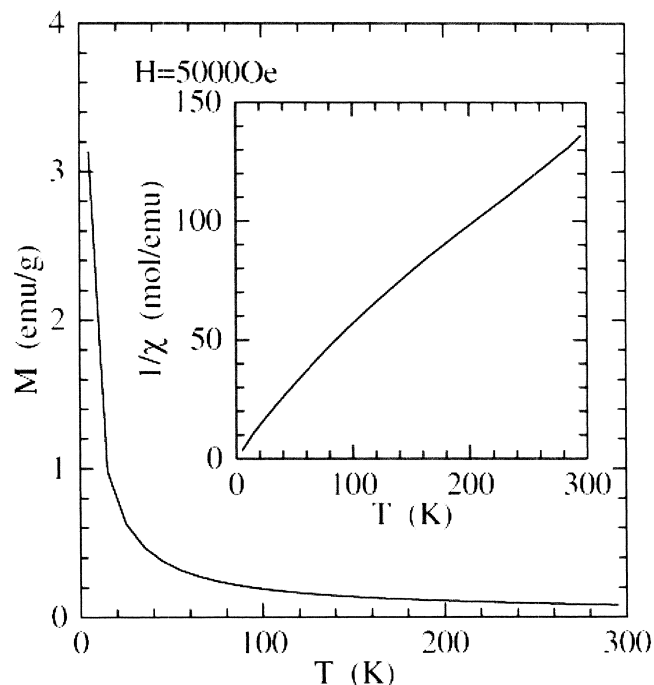


Fig. 6. Temperature dependence of the magnetization of $\text{NdRh}_3\text{B}_{1.000}$ in $H=5000$ Oe. The inset shows the temperature dependency of inverse susceptibility.

663 K and the final weight gain is 10.00%. The mixed phase of Rh and NdBO_3 is identified by XRD as a resultant product.

4. The micro-Vickers hardness is 4.9 ± 0.05 GPa for $\text{NdRh}_3\text{B}_{1.000}$.
5. $\text{NdRh}_3\text{B}_{1.000}$ shows a metallic temperature dependence of the resistivity down to 0.5 K.
6. Magnetic susceptibilities for $\text{NdRh}_3\text{B}_{1.000}$ show Curie-like paramagnetic behaviour due to Nd^{3+} moment. No trace of magnetic phase transitions and superconductivity is found down to 5 K.

Acknowledgements

This work was performed under the inter-university cooperative research program of the Laboratory for Advanced Materials (LAM), Institute for Materials Research (IMR), Tohoku University. The authors are grateful to Dr. K. Takada and Messrs. K. Obara, T. Sugawara, K. Sasaki, S. Tozawa, T. Takahashi, Y. Murakami and M. Ishikuro of IMR, Tohoku University, for help during sample preparations and chemical analyses.

References

- [1] L.D. Woolf, D.C. Johnston, H.B. MacKay, R.W. McCallum, M.B. Maple, *J. Low Temp. Phys.* 35 (1979) 651.
- [2] For a review, see Superconductivity in ternary compounds II, in: M.B. Maple, O. Fisher (Eds.), *Topics in Current Physics*, Vol. 34, Springer, Berlin, 1982.
- [3] T. Shishido, I. Higashi, H. Kitazawa, J. Bernhard, H. Takei, T. Fukuda, Boron, borides and related compounds, *Jpn. J. Appl. Phys.* 10 (Special issue) (1994) 142.
- [4] T. Shishido, K. Kudou, S. Okada, Y. Ye, M. Oku, H. Horiuchi, T. Fukuda, *J. Alloys Comp.* 280 (1998) 65.
- [5] H. Holleck, *J. Less-Common Metals* 52 (1977) 167.
- [6] P. Rogl, L. DeLong, *J. Less-Common Metals* 91 (1983) 97–102.
- [7] T. Shishido, J. Ye, K. Kudou, S. Okada, K. Obara, T. Sugawara, M. Oku, K. Wagatsuma, H. Horiuchi, T. Fukuda, *J. Alloys Comp.* 291 (1999) 52.
- [8] T. Shishido, J. Ye, K. Kudou, S. Okada, M. Oku, H. Horiuchi, T. Fukuda, *J. Ceram. Soc. Jpn.* 108 (7) (2000) 683.
- [9] R.E. Honig, *RCA Rev.* 23 (1962) 571.
- [10] G.V. Samsonov, I.M. Vinitskii, in: *Handbook of Refractory Compounds*, IFI/Plenum Press, New York, 1980, p. 303.